Atmos. Meas. Tech., 15, 11–19, 2022
https://doi.org/10.5194/amt-15-11-2022

Atmospheric Measurement Techniques
Open Access
EGU

A study on the fragmentation of sulfuric acid and dimethylamine clusters inside an atmospheric pressure interface time-of-flight mass spectrometer

Dina Alfaouri[1], Monica Passananti[1,2], Tommaso Zanca[1], Lauri Ahonen[1], Juha Kangasluoma[1], Jakub Kubečka[1], Nanna Myllys[3], and Hanna Vehkamäki[1]

[1]Department of Physics, Institute for Atmospheric and Earth System Research, University of Helsinki, Helsinki, 00014, Finland
[2]Dipartimento di Chimica, Università degli Studi di Torino, Via Pietro Giuria 5, Turin, 10125, Italy
[3]Department of Chemistry, University of Jyväskylä, Jyväskylä, 40014, Finland

Correspondence: Hanna Vehkamäki (hanna.vehkamaki@helsinki.fi)

Received: 23 June 2021 – Discussion started: 14 July 2021
Revised: 16 October 2021 – Accepted: 27 October 2021 – Published: 3 January 2022

Abstract. Sulfuric acid and dimethylamine vapours in the atmosphere can form molecular clusters, which participate in new particle formation events. In this work, we have produced, measured, and identified clusters of sulfuric acid and dimethylamine using an electrospray ionizer coupled with a planar-differential mobility analyser, connected to an atmospheric pressure interface time-of-flight mass spectrometer (ESI–DMA–APi-TOF MS). This set-up is suitable for evaluating the extent of fragmentation of the charged clusters inside the instrument. We evaluated the fragmentation of 11 negatively charged clusters both experimentally and using a statistical model based on quantum chemical data. The results allowed us to quantify the fragmentation of the studied clusters and to reconstruct the mass spectrum by removing the artifacts due to the fragmentation.

1 Introduction

Our climate is heavily impacted by atmospheric aerosol particles. These particles also play an important role in our daily lives. They determine the quality of the air we breathe and thus affect our health directly (Hirsikko et al., 2011; Zhao et al., 2021). The majority of particles in the Earth's atmosphere are formed from gaseous precursors. Both laboratory and field measurements indicate that sulfuric acid, often with various amines, acts as the main precursor for atmospheric new particle formation events by forming nanometre-scale clusters (Chen et al., 2012; Kürten et al., 2014; Mäkelä et al., 2001; Qiu and Zhang, 2013; Smith et al., 2010; Thomas et al., 2016; Zhao et al., 2011). In recent years, developments in high-resolution mass spectrometry have facilitated an increased understanding of the chemical composition, concentration, and stability of these molecular clusters. A central tool in detecting the elemental composition of these clusters is the chemical ionization atmospheric pressure interface time-of-flight mass spectrometer (CI–APi-TOF MS) (Jokinen et al., 2012; Yao et al., 2018). However, due to the lower stability of clusters in comparison to molecules, clusters are more susceptible to fragmentation and/or evaporation caused for example by ionization processes, low-pressure environments, and high-energy collisions inside the instrument. Previous studies have shown that theoretical models often predict higher cluster concentrations compared to APi-TOF measurements (Kurtén et al., 2011; Olenius et al., 2013). Cluster fragmentation processes inside the instrument (Olenius et al., 2013) have been speculated to be an explanation for this difference.

Our recent studies have made considerable progress in understanding the transformation of clusters inside the APi and in simulating collision-induced cluster fragmentation (CICF) (Passananti et al., 2019; Zanca et al., 2020; Zapadinsky et al., 2019). One of these studies (Passananti et al., 2019) investigated the fate of sulfuric acid trimer ions ($(H_2SO_4)_2HSO_4^-$)

inside an APi-TOF MS by exploring the effects of the voltages applied in the APi chambers on the CICF and identifying the regions of the APi in which the fragmentation is most likely to occur. Experimental results were found to be in good agreement with a theoretical model describing the CICF (Zapadinsky et al., 2019). This model simulates the motion of the charged clusters and the energy exchange with the carrier gas molecules inside the APi-TOF MS based on statistical principles combined with energy-level data from quantum chemical calculations. The simulated dynamics are defined by the electric fields inside the chambers of the instrument and the random collisions of the charged clusters with carrier gas molecules (Zapadinsky et al., 2019).

In this study, we extend our previous work to atmospherically relevant two-component clusters consisting of sulfuric acid and dimethylamine. Due to their varying size and shape, different clusters tend to have different electrical mobilities. We use a planar-differential mobility analyser (planar-DMA) (Amo-González and Pérez, 2018) to utilize this fact and select only one (known) cluster type at a time to enter the APi-TOF. We use an instrumental set-up (Fig. 1) consisting of an electrospray ionizer (ESI) and planar-DMA coupled with the APi-TOF MS.

Our main goals are to use this set-up to identify the clusters that are fragmented inside the APi-TOF MS and to quantify the fragmentation. We also compare our findings to theoretical fragmentation probabilities predicted by the CICF model (Zapadinsky et al., 2019). The combination of experimental and modelling data allows us to reconstruct a mass defect plot of the detected cluster ions, removing the artifacts due to the fragmentation.

2 Methodology

2.1 Experimental set-up

As mentioned above, the ESI is coupled with a DMA which is in turn connected to an electrometer and finally to the APi-TOF MS. The APi-TOF MS is an atmospheric pressure interface connected to a time-of-flight mass spectrometer (Tofwerk). The APi part acts as a guide for the ions and charged clusters from ambient pressure into high vacuum inside the TOF ($\sim 10^{-4}$ mbar). The TOF MS allows for the unambiguous identification of ion and cluster composition due to resolving power up to 3000 Th / Th (Junninen et al., 2010). Through the APi-TOF, charged clusters are subjected to a series of applied voltages (TOF power supply (TPS) voltages) which guide and focus them. These voltages hugely impact the fragmentation of the charged clusters and the instrument transmission.

Molecular ions are generated using an ESI from a solution of 100 mM / 100 mM dimethylamine / sulfuric acid in methanol and water with a ratio of $4:1\ v:v$. The sample is negatively charged using an electrode inserted into the liquid solution, and then the charged sample is electrosprayed into the planar-DMA model type P5 (by SEADM) with a sheath flow of N_2 carrier gas to separate charged clusters (with diameters up to a few nanometres) according to their electrical mobility. Thus, if we apply a certain voltage at the DMA, then only clusters of one electrical mobility will be passed onward. In the DMA two types of scans are conducted: full voltage scans and fixed voltage scans. Full voltage scans are done within a range of -900 to -2900 V with a voltage step of 5 V. Fixed voltage scans are done at the voltages where dimethylamine and sulfuric acid clusters appeared. Fixed voltage scans are done at the voltages where dimethylamine and sulfuric acid clusters appeared. Further details on the experimental procedure are found in the Supplement.

2.2 Cluster fragmentation simulation

We simulated the fragmentation of sulfuric acid and dimethylamine clusters using our statistical model (Zapadinsky et al., 2019). As mentioned above, this model describes the motion of the charged clusters through the APi-TOF MS and the energy exchange caused by collisions between the charged clusters and the carrier gas molecules. These collisions may cause the fragmentation of the cluster ions inside the instrument if they convey a sufficient amount of energy (Zapadinsky et al., 2019). The model needs as input data on the experimental conditions (temperature and voltages and pressures inside the APi chambers) and information about the (vibrational and rotational) energy levels which are used to evaluate the densities of states. These latter were obtained using quantum chemistry data from calculations carried out within our group (Myllys et al., 2019), where vibrational frequency analyses were carried out at the ωB97X-D/6-31++G(d,p) level of theory. Further details on the model and quantum chemistry calculations are given in the Supplement.

3 Results and discussion

Figure 2 shows a 2D plot of the combined and synchronized signals from the DMA and the APi-TOF MS, with the DMA voltage on the x axis, the cluster mass / charge ratio on the y axis, and the signal intensity on a colour scale. This type of data visualization allows us to evaluate the presence of multicharged compounds, the presence of fragmented clusters, and the range of m/z and mobility of the clusters produced in the ESI. Indeed, this plot gives a convenient overview of the cluster fragmentation in the (negatively charged) sulfuric acid–dimethylamine system. For a given DMA voltage, in an ideal situation only singly charged clusters with a unique elemental composition (and thus mass) enter the APi-TOF MS. In the absence of fragmentation, this should result in one narrow peak in the mass spectrum and thus only one line in the 2D plot. Any deviation from this means that there are either

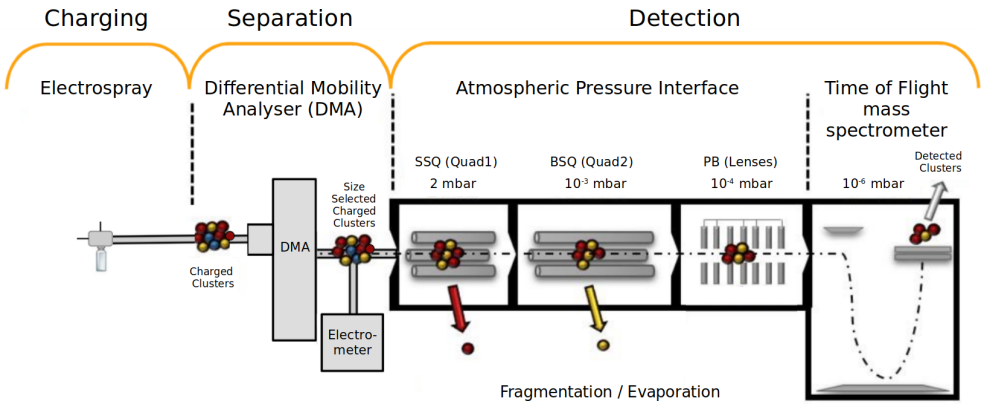

Figure 1. Schematic figure (not to scale) representing the experimental set-up of an electrospray ionizer and planar-differential mobility analyser, connected to an atmospheric pressure interface time-of-flight mass spectrometer (ESI–DMA–APi-TOF MS). Figure modified from Passananti et al. (2019).

multi-charged clusters, singly charged clusters with different masses with the same mobility, and/or cluster fragmentation. As seen in Fig. 2, in our experimental conditions, the groups of peaks present are concentrated largely along one linear line, which means that we mainly observe singly charged clusters. In case of multi-charged clusters in 2D plots, several groups of peaks are concentrated along different linear lines (one line for each charge state); as an example of multi-charged 2D plots, see Fig. 1b in Larriba et al. (2014). Moreover, considering our sample composition and the resolution of the DMA, the likelihood of detecting singly charged clusters with different masses with the same mobilities are low. This leaves us with cluster fragmentation, which can be highlighted from the 2D plots.

If a cluster, upon entering the APi-TOF, becomes fragmented, multiple signals are seen at the same voltage but at different mass / charge ratios. In Fig. 2, an example of a cluster and its fragment are shown (circled by dashed red lines). Moreover, upon entering the APi-TOF MS, several clusters undergo neutral evaporation or fragmentation, especially when the produced cluster or ion is a highly stable one. This could result in continuous horizontal lines as seen in Fig. 2 for the 1B ion where $\mathrm{M1B} \rightarrow \mathrm{M} + 1\mathrm{B}$ (M is an arbitrary cluster).

Using the full voltage scan mode, it is possible to detect all negatively charged clusters of dimethylamine and sulfuric acid produced by the ESI within the scanned DMA voltage range given the APi-TOF transmission is good enough. To identify sulfuric acid–dimethylamine clusters, the MS data have been analysed, and clusters are reported in Fig. 3. In particular, Fig. 3 shows a mass defect plot of all 11 dimethylamine and sulfuric acid charged clusters produced and detected in our system. Other clusters or impurities are not shown in the figure as they are not relevant for this study. The DMA voltages and the m/z values for each detected cluster are reported in Table S3 of the Supplement. For simplicity, throughout the whole paper we refer to sulfuric acid as S, dimethylamine as D, bisulfate ion as B, and clusters as for example 2D2S1B, which corresponds to a cluster of two dimethylamine molecules, two sulfuric acid molecules, and one bisulfate ion. The majority of the charged clusters had either a $1:1$ ratio of sulfuric acid and dimethylamine with a bi-sulfate ion attached or a $N+1:N$ ratio, i.e. with one more sulfuric acid than dimethylamine molecule (in addition to the bi-sulfate ion). The smallest detected $1:1$ ratio cluster is 2D2S1b; we do not observe the 1D1S1B cluster, probably due to its lower stability compared to a larger cluster. This is in agreement with the computed trend of stability of negatively charged sulfuric acid–dimethylamine clusters (Myllys et al., 2019). Moreover, our detected clusters are similar to those detected in a previous study of the same sulfuric acid and dimethylamine solution (Thomas et al., 2016) produced in gas-phase chamber experiments (Almeida et al., 2013; Kürten et al., 2014) and in ambient measurements (Yao et al., 2018).

The full voltage scan and the 2D plot (Fig. 2) are useful for providing a fast qualitative interpretation of the data. However, for an in-depth analysis of the data and a quantitative measure of the fragmentation or survival probability of each cluster type, experiments with fixed voltage and longer data acquisition times are needed. In a fixed voltage scan experiment a single cluster type is selected, and the mass spectrum is recorded for that specific cluster. We performed fixed voltage scan experiments for each cluster type to identify the fragmentation pathways and quantify the survival probability. For the clusters not fragmented inside the APi, only the signal of the original cluster is observed in the mass spectrum. In case of fragmentation, two or more signals are observed in the mass spectrum. For the larger clusters, we observed several fragmentation pathways. Figure 4 shows the MS spectrum of the fixed scan experiment for cluster 1D2S1B as an example. In the MS spectrum there is the signal of the original cluster (1D2S1B) at 337.95 Th, and there are three signals at lower m/z representing a frag-

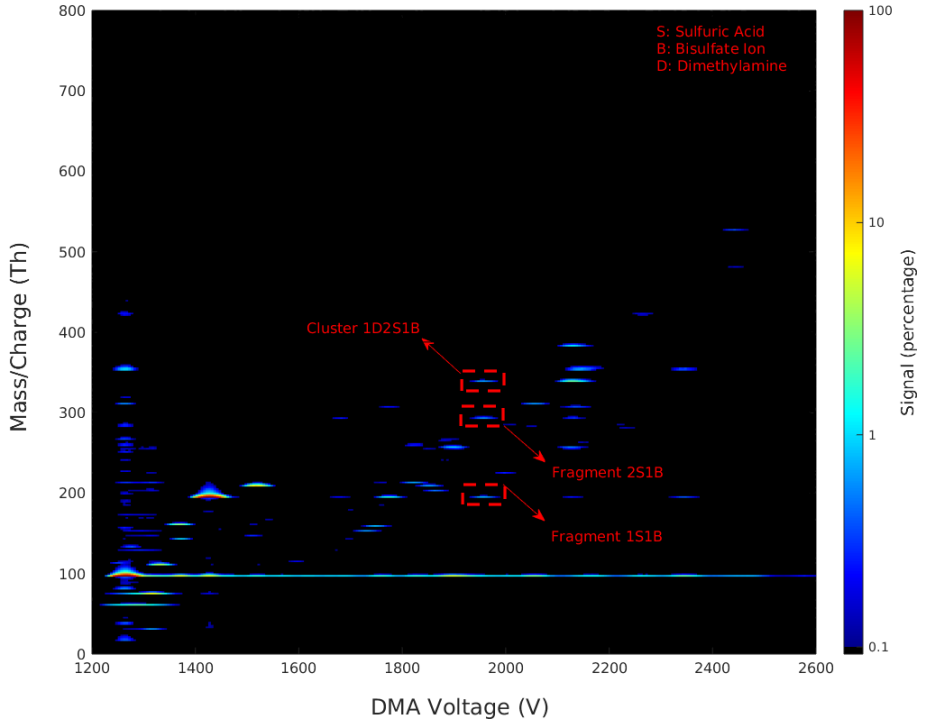

Figure 2. The 2D plot of the differential mobility spectrum and the mass spectrum of negatively charged sulfuric acid and dimethylamine clusters generated by the ESI. The plot shows the mass / charge versus the DMA voltage with the signal intensity as a colour scale. Dashed red lines highlight the fragmentation of cluster 1D2S1B and its fragments 2S1B and 1S1B as an example, where D is dimethylamine, S is sulfuric acid, and B is bisulfate ion.

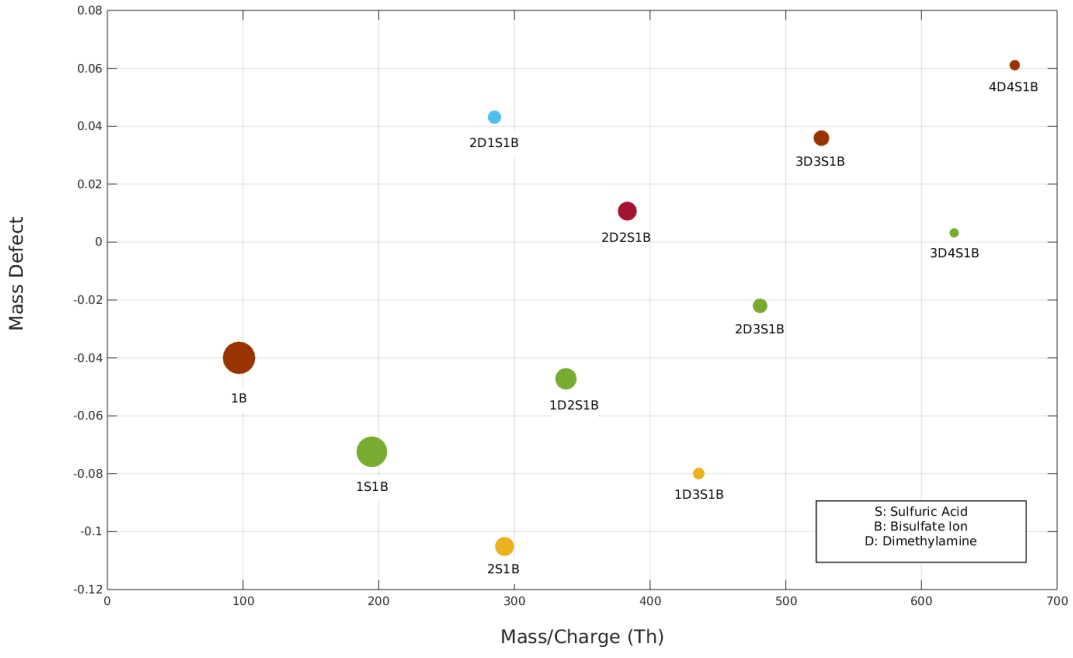

Figure 3. The mass defect plot of sulfuric acid and dimethylamine clusters detected by the APi-TOF MS. The circle size reflects the intensity of the detected clusters. Clusters of the same colour have the same sulfuric acid : dimethylamine ratio.

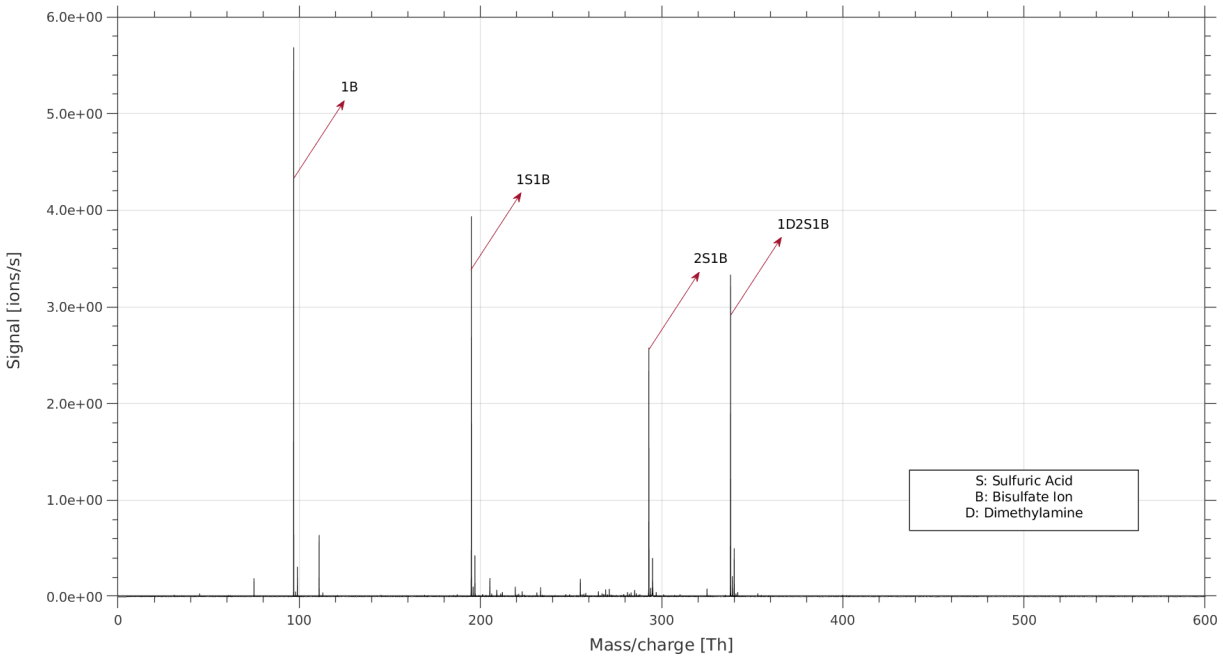

Figure 4. The MS spectrum of the fixed scan experiment for cluster 1D2S1B.

mented cluster. Each signal is a cluster deriving from a different fragmentation pathway, and 1D2S1B can fragment via these three pathways.

$$1D2S1B \rightarrow 2S1B + 1D \quad \text{(R1)}$$

$$1D2S1B \rightarrow 1S1B + 1S1D \quad \text{(R2)}$$

$$1D2S1B \rightarrow 1B + 1D2S \quad \text{(R3)}$$

We calculated the overall survival probability of 1D2S1B (using the ratio between the signal intensity of the parent cluster and the sum of the parent and fragmented clusters; all signal intensities have been corrected by the mass-dependent transmission of the APi-TOF) and the probability of fragmentation for each pathway. We also take into account an average background signal of the 1B ion (seen as a horizontal line in Fig. 2).

The fragmentation region inside the APi is relatively short (Passananti et al., 2019), and the daughter clusters are likely to leave this region before having a chance to fragment again, and thus we ignore subsequent fragmentation events. The fragmentation pathways and the survival probability for each cluster are reported in the Supplement.

We compared experimental data with the survival probabilities calculated with the CICF model to understand the fragmentation processes. To simulate the CICF inside an APi-TOF, we needed to define all fragmentation pathways for each studied cluster. However, only single fragmentation pathways can be considered for each specific simulation. To identify the most probable fragmentation pathways, we computed the reaction (kinetic) rate constants at different internal energies of the cluster for each possible fragmentation pathway and selected the pathways with the highest rate constants at the typical/average internal energy (see the Supplement for more detailed information). All clusters except 1S1B may fragment through at least two different pathways, and the number of pathways increases with the cluster size. Finally we calculated an overall survival probability for each cluster using the selected most probable fragmentation pathways.

Figure 5 shows the comparison of the overall survival probability according to experiments and model simulations for all studied clusters. For most of the clusters detected, the experimental and model results of the survival probability are in good agreement. There can be several reasons for the discrepancies in the survival probability between the experiments and the model.

1. For some parent clusters multiple fragmentation pathways can occur simultaneously within the same experiment.

2. The fragmentation of a multi-charged cluster with the same mobility as a different singly charged cluster can produce the same fragments, which leads to an underestimation of the experimental survival probability of the studied singly charged cluster.

3. Clusters with mobility peaks very close to each other can have overlapping signals which are difficult to separate.

For most of the clusters the model underestimates the survival probability compared to the experimental results, which could be explained by reason 1 and/or 2 in the list above.

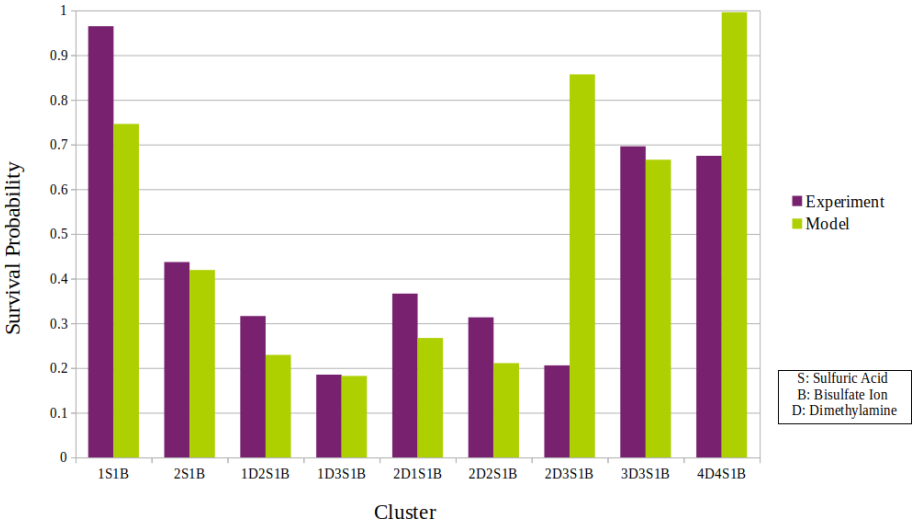

Figure 5. The overall survival probability of all sulfuric acid–dimethylamine clusters detected and calculated experimentally versus that simulated and calculated by our statistical model.

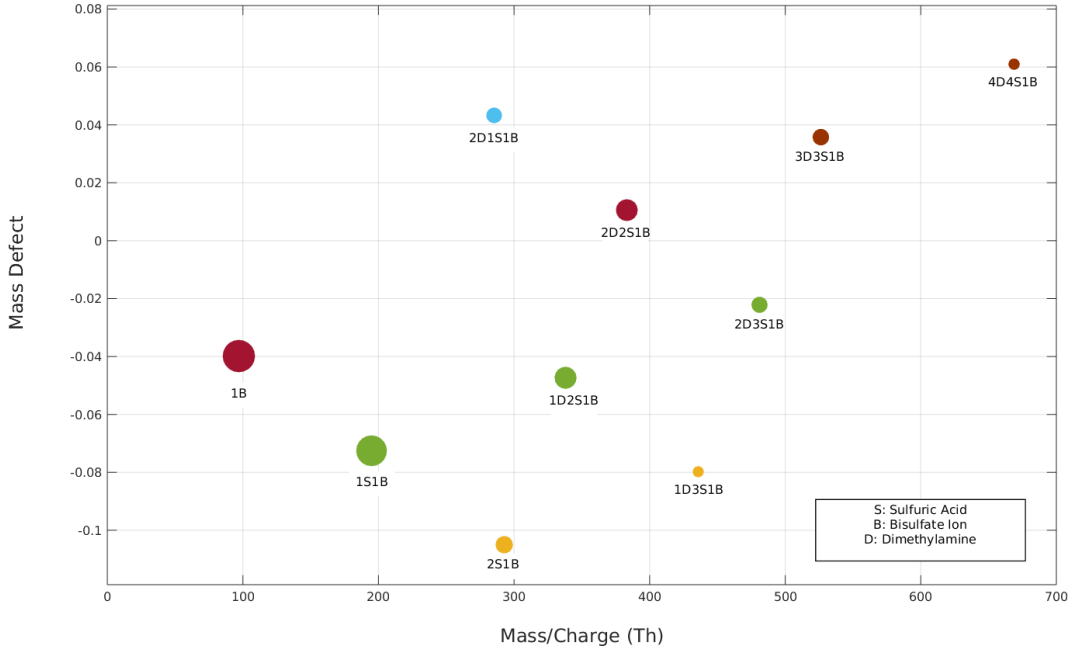

Figure 6. The reconstructed mass defect versus mass / charge (Th) plot based on that shown in Fig. 3 after accounting for all fragmentation processes. Note that cluster 3D4S1B is not seen here as it is only a fragmented product of cluster 4D4S1B.

Only for clusters 2D3S1B and 4D4S1B does the model overestimate the survival probability, and for these clusters there is a large discrepancy between the model and the experiments. The reason for this discrepancy might be the harmonic potential description of the vibrations used in deriving the energy levels of the cluster from quantum chemistry. For large clusters, ignoring the anharmonicity may result in overestimates for the survival probability. On the one hand, the trend in clusters 2D2S1B, 3D3S1B, and 4D4S1B could be explained by this increasing role of anharmonicity with cluster size, while 2D3S1B does not fit to this trend, probably due to different ratios of dimethylamine to sulfuric acid molecules. 2D3S1B has fewer hydrogen bonds since there are only two dimethylamine molecules in the cluster: this corresponds to a weaker bond network which may lead to a higher uncertainty. In addition to that, as indicated by Table S1 in the Supplement, more simultaneous fragmentation pathways were experimentally observed for cluster 2D3S1B in comparison to all the other clusters. This contributes to a higher uncertainty in the experimental survival probability

calculation for this cluster. Thus, the larger discrepancy for the 2D3S1B cluster could be a combined reason for both the experimental and model uncertainty in the evaluation of the survival probability.

Knowing the instrumental transmission (see Supplement Sect. S6), cluster fragmentation pathways and survival probabilities allow for reconstruction of the mass defect plot, removing the effects of fragmentation (Fig. 6). In particular, the intensity of a cluster was increased in case it has a survival probability lower than 1 and/or decreased if it was produced as a result of a fragmentation of another cluster. More details on the procedure to reconstruct the mass defect plot are reported in the Supplement. This procedure enables the removal of artifacts due to the fragmentation of clusters and gives more accurate information about the actual concentration and composition of detected clusters.

4 Conclusion

In this work we tested our experimental set-up (ESI–DMA–APi-TOF MS), which consists of two high-resolution instruments, and a first-principle-based CICF model to study the fragmentation of atmospheric-relevant clusters. We generated and identified 11 charged sulfuric acid and dimethylamine clusters, and for each of these clusters, we quantified the extent of the fragmentation inside the instrument both experimentally and using a statistical model. The results showed a good agreement between the experiment and the model, shedding light on the nature of the fragmentation processes within this instrument. Our study revealed that larger clusters may undergo multiple fragmentation pathways. Our data allowed us to reconstruct the mass spectrum (i.e. a mass defect plot) of the identified clusters, so that we were able to define the original signal intensities of the detected clusters as if they had remained intact inside the instrument, removing artifacts due to the fragmentation. In the future, we anticipate that these proof-of-concept results can be extended also to other cluster-forming systems, and fragmentation corrections could be incorporated into standard data-analysis tools related to these instruments. This kind of sophisticated data analysis would significantly increase the accuracy of atmospheric cluster measurements, allowing for a better understanding of the conditions that lead to new particle formation.

Data availability. The data are publicly available in a GitHub repository (https://github.com/DinaAlfaouri/A-study-on-the-fragmentation-of-atmospheric-clusters-inside-an-APi-TOF-MS/tree/v1.12.21, last access: 23 December 2021; https://doi.org/10.5281/zenodo.5801564, Alfaouri, 2021).

Supplement. The supplement related to this article is available online at: https://doi.org/10.5194/amt-15-11-2022-supplement.

Author contributions. HV came up with the research idea. DA performed the experiments, data analysis, and result interpretation and wrote the first draft of the paper. MP helped in planning the project, supervising the experiments, analysing the data, interpreting the results, and writing the paper. JaK and NM performed the quantum chemistry calculations and wrote the parts about those calculations. TZ helped in performing the simulations of the fragmentation model, interpreting the model simulation results, and writing the parts about the model. LA helped in the interpretation of the results and by providing the code that visualizes the synchronized data. JuK helped in the interpretation of the results. All the authors contributed to the writing of this paper.

Competing interests. The contact author has declared that neither they nor their co-authors have any competing interests.

Disclaimer. Publisher's note: Copernicus Publications remains neutral with regard to jurisdictional claims in published maps and institutional affiliations.

Acknowledgements. We thank the ERC Project 692891-DAMOCLES, Academy of Finland project 1325656, University of Helsinki Faculty of Science ATMATH Project, for funding, and the CSC-IT Center for Science in Espoo, Finland, for computational resources. We acknowledge Evgeni Zapadinsky for all his help, knowledge, discussions and his expert advice. We also acknowledge Theo Kurtén for his expert advice.

Financial support. This research has been supported by the European Research Council, H2020 European Research Council (DAMOCLES (grant no. 692891)), the University of Helsinki Faculty of Science (ATMATH Project), and the Academy of Finland (project no. 1325656).

Open-access funding was provided by the Helsinki University Library.

Review statement. This paper was edited by Daniela Famulari and reviewed by three anonymous referees.

References

Alfaouri, D.: DinaAlfaouri/A-study-on-the-fragmentation-of-atmospheric-clusters-inside-an-APi-TOF-MS: DinaAlfaouri/A-study-on-the-fragmentation-of-atmospheric-clusters-inside-an-APi-TOF-MS (v1.12.21), Zenodo [data set], https://doi.org/10.5281/zenodo.5801564, 2021.

Almeida, J., Schobesberger, S., Kürten, A., Ortega, I. K., Kupiainen-Määttä, O., Praplan, A. P., Adamov, A., Amorim, A., Bianchi, F., Breitenlechner, M., David, A., Dommen, J., Donahue, N. M., Downard, A., Dunne, E., Duplissy, J., Ehrhart, S., Flagan, R. C., Franchin, A., Guida, R., Hakala, J., Hansel, A.,

Heinritzi, M., Henschel, H., Jokinen, T., Junninen, H., Kajos, M., Kangasluoma, J., Keskinen, H., Kupc, A., Kurtén, T., Kvashin, A. N., Laaksonen, A., Lehtipalo, K., Leiminger, M., Leppä, J., Loukonen, V., Makhmutov, V., Mathot, S., McGrath, M. J., Nieminen, T., Olenius, T., Onnela, A., Petäjä, T., Riccobono, F., Riipinen, I., Rissanen, M., Rondo, L., Ruuskanen, T., Santos, F. D., Sarnela, N., Schallhart, S., Schnitzhofer, R., Seinfeld, J. H., Simon, M., Sipilä, M., Stozhkov, Y., Stratmann, F., Tomé, A., Tröstl, J., Tsagkogeorgas, G., Vaattovaara, P., Viisanen, Y., Virtanen, A., Vrtala, A., Wagner, P. E., Weingartner, E., Wex, H., Williamson, C., Wimmer, D., Ye, P., Yli-Juuti, T., Carslaw, K. S., Kulmala, M., Curtius, J., Baltensperger, U., Worsnop, D. R., Vehkamäki, H., and Kirkby, J.: Molecular understanding of sulphuric acid–amine particle nucleation in the atmosphere, Nature, 502, 359–363, https://doi.org/10.1038/nature12663, 2013.

Amo-González, M. and Pérez, S.: Planar Differential Mobility Analyzer with a Resolving Power of 110, Anal. Chem., 90, 6735–6741, https://doi.org/10.1021/acs.analchem.8b00579, 2018.

Chen, M., Titcombe, M., Jiang, J., Jen, C., Kuang, C., Fischer, M. L., Eisele, F. L., Siepmann, J. I., Hanson, D. R., Zhao, J., and McMurry, P. H.: Acid-base chemical reaction model for nucleation rates in the polluted atmospheric boundary layer, P. Natl. Acad. Sci. USA, 109, 18713–18718, https://doi.org/10.1073/pnas.1210285109, 2012.

Hirsikko, A., Nieminen, T., Gagné, S., Lehtipalo, K., Manninen, H. E., Ehn, M., Hõrrak, U., Kerminen, V.-M., Laakso, L., McMurry, P. H., Mirme, A., Mirme, S., Petäjä, T., Tammet, H., Vakkari, V., Vana, M., and Kulmala, M.: Atmospheric ions and nucleation: a review of observations, Atmos. Chem. Phys., 11, 767–798, https://doi.org/10.5194/acp-11-767-2011, 2011.

Jokinen, T., Sipilä, M., Junninen, H., Ehn, M., Lönn, G., Hakala, J., Petäjä, T., Mauldin III, R. L., Kulmala, M., and Worsnop, D. R.: Atmospheric sulphuric acid and neutral cluster measurements using CI-APi-TOF, Atmos. Chem. Phys., 12, 4117–4125, https://doi.org/10.5194/acp-12-4117-2012, 2012.

Junninen, H., Ehn, M., Petäjä, T., Luosujärvi, L., Kotiaho, T., Kostiainen, R., Rohner, U., Gonin, M., Fuhrer, K., Kulmala, M., and Worsnop, D. R.: A high-resolution mass spectrometer to measure atmospheric ion composition, Atmos. Meas. Tech., 3, 1039–1053, https://doi.org/10.5194/amt-3-1039-2010, 2010.

Kürten, A., Jokinen, T., Simon, M., Sipilä, M., Sarnela, N., Junninen, H., Adamov, A., Almeida, J., Amorim, A., Bianchi, F., Breitenlechner, M., Dommen, J., Donahue, N. M., Duplissy, J., Ehrhart, S., Flagan, R. C., Franchin, A., Hakala, J., Hansel, A., Heinritzi, M., Hutterli, M., Kangasluoma, J., Kirkby, J., Laaksonen, A., Lehtipalo, K., Leiminger, M., Makhmutov, V., Mathot, S., Onnela, A., Petäjä, T., Praplan, A. P., Riccobono, F., Rissanen, M. P., Rondo, L., Schobesberger, S., Seinfeld, J. H., Steiner, G., Tomé, A., Tröstl, J., Winkler, P. M., Williamson, C., Wimmer, D., Ye, P., Baltensperger, U., Carslaw, K. S., Kulmala, M., Worsnop, D. R., and Curtius, J.: Neutral molecular cluster formation of sulfuric acid–dimethylamine observed in real time under atmospheric conditions, P. Natl. Acad. Sci. USA, 111, 15019–15024, https://doi.org/10.1073/pnas.1404853111, 2014.

Kurtén, T., Petäjä, T., Smith, J., Ortega, I. K., Sipilä, M., Junninen, H., Ehn, M., Vehkamäki, H., Mauldin, L., Worsnop, D. R., and Kulmala, M.: The effect of H_2SO_4 – amine clustering on chemical ionization mass spectrometry (CIMS) measurements of gas-phase sulfuric acid, Atmos. Chem. Phys., 11, 3007–3019, https://doi.org/10.5194/acp-11-3007-2011, 2011.

Larriba, C., de la Mora, J. F., and Clemmer, D. E.: Electrospray Ionization Mechanisms for Large Polyethylene Glycol Chains Studied Through Tandem Ion Mobility Spectrometry, J. Am. Soc. Mass Spectrom., 25, 1332–1345, https://doi.org/10.1007/s13361-014-0885-0, 2014.

Mäkelä, J. M., Yli-Koivisto, S., Hiltunen, V., Seidl, W., Swietlicki, E., Teinilä, K., Sillanpää, M., Koponen, I. K., Paatero, J., Rosman, K., and Hämeri, K.: Chemical composition of aerosol during particle formation events in boreal forest, Tellus B, 53, 380–393, https://doi.org/10.3402/tellusb.v53i4.16610, 2001.

Myllys, N., Kubečka, J., Besel, V., Alfaouri, D., Olenius, T., Smith, J. N., and Passananti, M.: Role of base strength, cluster structure and charge in sulfuric-acid-driven particle formation, Atmos. Chem. Phys., 19, 9753–9768, https://doi.org/10.5194/acp-19-9753-2019, 2019.

Olenius, T., Schobesberger, S., Kupiainen-Määttä, O., Franchin, A., Junninen, H., Ortega, I. K., Kurtén, T., Loukonen, V., Worsnop, D. R., Kulmala, M., and Vehkamäki, H.: Comparing simulated and experimental molecular cluster distributions, Faraday Discuss., 165, 75–89, https://doi.org/10.1039/c3fd00031a, 2013.

Passananti, M., Zapadinsky, E., Zanca, T., Kangasluoma, J., Myllys, N., Rissanen, M. P., Kurtén, T., Ehn, M., Attoui, M., and Vehkamäki, H.: How well can we predict cluster fragmentation inside a mass spectrometer?, Chem. Commun., 55, 5946–5949, https://doi.org/10.1039/C9CC02896J, 2019.

Qiu, C. and Zhang, R.: Multiphase chemistry of atmospheric amines, Phys. Chem. Chem. Phys., 15, 5738, https://doi.org/10.1039/c3cp43446j, 2013.

Smith, J. N., Barsanti, K. C., Friedli, H. R., Ehn, M., Kulmala, M., Collins, D. R., Scheckman, J. H., Williams, B. J., and McMurry, P. H.: Observations of aminium salts in atmospheric nanoparticles and possible climatic implications, P. Natl. Acad. Sci. USA, 107, 6634–6639, https://doi.org/10.1073/pnas.0912127107, 2010.

Thomas, J. M., He, S., Larriba-Andaluz, C., DePalma, J. W., Johnston, M. V., and Hogan Jr., C. J.: Ion mobility spectrometry-mass spectrometry examination of the structures, stabilities, and extents of hydration of dimethylamine–sulfuric acid clusters, Phys. Chem. Chem. Phys., 18, 22962–22972, https://doi.org/10.1039/C6CP03432B, 2016.

Yao, L., Garmash, O., Bianchi, F., Zheng, J., Yan, C., Kontkanen, J., Junninen, H., Mazon, S. B., Ehn, M., Paasonen, P., Sipilä, M., Wang, M., Wang, X., Xiao, S., Chen, H., Lu, Y., Zhang, B., Wang, D., Fu, Q., Geng, F., Li, L., Wang, H., Qiao, L., Yang, X., Chen, J., Kerminen, V.-M., Petäjä, T., Worsnop, D. R., Kulmala, M., and Wang, L.: Atmospheric new particle formation from sulfuric acid and amines in a Chinese megacity, Science, 361, 278–281, https://doi.org/10.1126/science.aao4839, 2018.

Zanca, T., Kubečka, J., Zapadinsky, E., Passananti, M., Kurtén, T., and Vehkamäki, H.: Highly oxygenated organic molecule cluster decomposition in atmospheric pressure interface time-of-flight mass spectrometers, Atmos. Meas. Tech., 13, 3581–3593, https://doi.org/10.5194/amt-13-3581-2020, 2020.

Zapadinsky, E., Passananti, M., Myllys, N., Kurtén, T., and Vehkamäki, H.: Modeling on Fragmentation of Clusters inside a Mass Spectrometer, J. Phys. Chem. A, 123, 611–624, https://doi.org/10.1021/acs.jpca.8b10744, 2019.

Zhao, J., Smith, J. N., Eisele, F. L., Chen, M., Kuang, C., and McMurry, P. H.: Observation of neutral sulfuric acid-amine containing clusters in laboratory and ambient measurements, Atmos. Chem. Phys., 11, 10823–10836, https://doi.org/10.5194/acp-11-10823-2011, 2011.

Zhao, J., Birmili, W., Hussein, T., Wehner, B., and Wiedensohler, A.: Particle number emission rates of aerosol sources in 40 German households and their contributions to ultrafine and fine particle exposure, Indoor Air, 31, 818–831, https://doi.org/10.1111/ina.12773, 2021.